ELECTROSTATICALLY ACTUATED DEPLOYMENT FOR CLOSE-PROXIMITY LEADER-FOLLOWER FORMATION IN LEO PLASMA WAKES

Jordan Maxwell * **and Hanspeter Schaub** †

The feasibility of using electrostatic actuation to deploy a daughter craft from its mother into a close-proximity leader-follower formation is investigated. The mother craft is equipped with a set of affixed spheres whose charge is modulated to hold the spherical charged follower craft along a proscribed trajectory to its nominal leader-relative position. All charged objects are constrained to remain in the plasma wake generated behind all LEO craft because the more-dense ambient plasma outside the wake prevents object charging and electric field propagation. Once deployment is achieved, a controlled electric field is generated by the leader to counter relative accelerations from perturbations like differential drag and solar radiation pressure, holding the follow in its nominal position. An optimal controller is derived for the system described, incorporating Coulomb accelerations and linearized gravity and drag accelerations. Simulations are run under unmodeled perturbations and sensor noise for various trajectories, demonstrating the challenges and benefits associated with the technique. Finally, the control authority and power requirements are considered. It is shown that, for this control methodology, the overall effort is highly dependent on the chosen trajectory.

INTRODUCTION

Many next-generation missions require formation flying. Capabilities including Space Situational Awareness (SSA), spacecraft servicing,[1] debris mitigation, and Earth observation benefit from or rely on two craft operating in close-proximity to one another. Modern guidance, navigation, and control techniques are ill-suited to highly precise station keeping, as the use of traditional or low-thrust propulsion increases mission mass and cost and introduces challenges such as plume impingement on neighboring craft. However, by actively charging two resident space objects (RSOs) and utilizing concepts from differential drag formation flight, relative position and attitude control can be achieved with high fuel efficiency.

Currently, close-proximity operations such as docking apply impulsive thrusters as actuators. The CanX-4/5 dual spacecraft experiment utilized a pair of nanosatellites to achieve sub-meter level control accuracy while using between 1.15 and 3.40 cm/s of ΔV per orbit.[2] While these values are small, they imply that a multi-year formation flight mission would require hundreds of meters per second of ΔV, which would require steep trade-offs from other mission areas. Therefore, alternative fuel-efficient formation keeping technologies must be developed to enable next-generation mission concepts.

One zero-propellant technology is electrostatic actuation — a technique that uses charge accumulated on two RSO's surfaces to generate Coulomb accelerations for relative position and attitude control. Originally developed for the Geosynchronous Earth Orbit (GEO) regime, the technique has recently been adapted for use in the plasma wakes behind Low Earth Orbit — a region with plasma conditions conducive to vehicle charging

*Graduate Research Assistant, Department of Aerospace Engineering Sciences, University of Colorado, 431 UCB, Colorado Center for Astrodynamics Research, Boulder, CO 80309-0431

†Glenn L. Murphy Endowed Chair, Department of Aerospace Engineering Sciences, University of Colorado, 431 UCB, Colorado Center for Astrodynamics Research, Boulder, CO 80309-0431

and force and torque propagation.[3] The wake exhibits decreased neutral density, so a craft flying in another's wake will experience relative accelerations due to differential drag. By generating equal and opposite relative Coulomb accelerations, simulations indiciate that a follower craft can be held to some nominal position within 1 cm.[?]

This work applies the proposed drag-balanced Coulomb formation flying concept to a more complicated mission scenario. This paper present novel results in the field of electrostatic actuation by demonstrating that highly-precise formation keeping and maneuvers can be accomplished in LEO-like conditions using reasonably small craft potentials, even under significant perturbations.

PROBLEM STATEMENT

A two-spacecraft, along-track formation in Low Earth Orbit (LEO) is considered in this work, which aims to study the feasibility of coulomb-balanced differential-drag formation flight in LEO spacecraft wakes. The Displaced Phase Center Antenna (DPCA)[4,5] concept is used as a frame for this investigation, providing notional mission scenario parameters as well as one of several motivations for the development of the proposed technique. Prior studies in DPCA mission design have shown a required baseline offset on the order of meters — providing a configuration appropriate to the volumetric constraints of a typical LEO plasma wake — with this relative rectilinear position being held to sub-centimeter accuracy. These parameters are considered as bounding constraints to inform the parameters considered by this study.

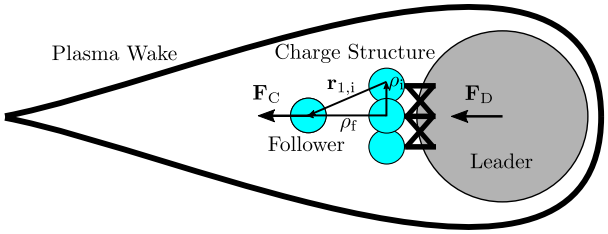

Figure 1. Illustration of the Coulomb-balanced differential drag concept

The mission concept is illustrated in Figure 1. A charge structure consisting of n_{cs} spheres equally spaced in angle about a circle of radius r_{cs} is attached to the rear of the leader craft. This configuration creates an electrostatic potential well behind the leader craft, which is pictured in terms of an electric field in Figure 2.

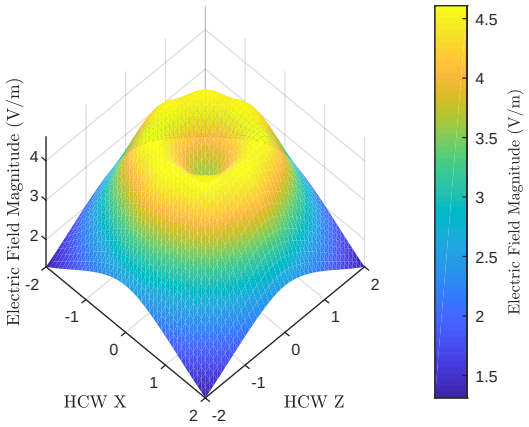

Figure 2. The electric field 1 m behind the charge structure for a configuration in which n_{cs} = 8, r_{cs} = 1 m

A charged follower craft is deployed from the leader craft to a nominal position ρ_{f} along a proscribed trajectory. A feedback law generates the charges on each sphere in Figure 1 such that the follower remains on the chosen trajectory under differential drag and unmodeled perturbations. Once the desired position is reached, the follower nominally sits directly in the center of the electrostatic potential well in Figure 2, so that only along the HCW Y axis is a repulsive force felt. Should any unmodeled perturbation provide off-axis accelerations, the structure of the potential well naturally provides a restoring acceleration, though control is also applied in such a case to correct displacements.

Because the wake exhibits decreased neutral density as well as plasma density, the drag acceleration on the follower is assumed to be zero. Differential drag will always decrease the separation between the leader and follower in this case, so voltages are sourced on the follower and charge structure to cancel the drag acceleration of the leader. Negative voltages are chosen because the wake is only ion devoid — the presence of electrons means that negative voltages will require less power than positive ones. Additionally, shielding of negatively signed potentials in an electron-dominated plasma is significantly less than that of those positive.[6] Therefore, the wake acts as vacuum for negative potentials. A "pusher-only" control is used in which the controller only ever sources repulsive Coulomb forces. If the follower exceeds the nominal separation, the voltages are nulled and differential drag brings the craft back together. For this investigation, it is assumed beforehand that the extremely tight DCPA-imposed tolerance on relative position will also require the craft to remain in the wake — it is demonstrated in later sections that this is indeed the case. This investigation focuses on feasibility of the mission concept and control scheme and, as such, the wake is taken to behave as vacuum. This assumption is validated in part by Durand de Gevigney et. al, but the effects on wake geometry and properties resulting from placing charged objects within are outside the scope of this preliminary study and are therefore neglected.

MSM is applied to calculate the Coulomb acceleration between the leader and follower crafts. This modeling method is especially well-suited to the propose technique, given the arrangement of charged spheres. However, for simplicity and computational efficiency, nearby charge spheres are considered as point sources for all mutual effects. The higher-order effects resulting from complicated charge distributions are again considered out-of-scope for this study.

NONLINEAR EQUATIONS OF MOTION

Three perturbations are included in the simplified model used throughout this investigation: Two-body gravity, orbital drag, and Coulomb forces. The Hill-Clohessy-Whiltshire (HCW) frame is used with the origin at the center of the charge structure attached to the leader. Therefore, the accelerations of the follower relative to the leader (stationary in the HCW frame) are used throughout.

$$^{\mathcal{H}}\boldsymbol{\rho} = [\mathcal{N}\mathcal{H}]\left(^{\mathcal{N}}\boldsymbol{r}_{\mathrm{f}} - {}^{\mathcal{N}}\boldsymbol{r}_{\mathrm{L}}\right) \tag{1}$$

Henceforth, the left superscript on $\boldsymbol{\rho}$ and its derivatives is suppressed. The state of the system is defined $\boldsymbol{X} = [\boldsymbol{\rho}, \dot{\boldsymbol{\rho}}]^T$ and evolves according to the equation

$$\dot{\boldsymbol{X}} = \boldsymbol{F}(\boldsymbol{X}, \boldsymbol{V}) \tag{2}$$

where $\boldsymbol{F}$ is a non-linear vector function of the state and charges $\boldsymbol{Q}$ which, in this case, incorporates two-body gravity, atmospheric drag, and Coulomb forces.

Under the assumptions of a circular leader orbit and nearby follower orbit, the formulation of the HCW equations with linearized drag forces presented first by Silva[7] and modified by Harris[8] is applied. These equations of motion typically include a secular differential drag acceleration which in this case is assumed to be canceled by the Coulomb repulsion between the leader and follower. These linearized descriptions are incorporated into the control formulation discussed in later sections, while the full dynamics are implemented when simulating the system dynamics.

Coulomb Acceleration

The Coulomb acceleration of the follower relative to the leader is calculated from the charge on the follower and the electric field of the leader. It is assumed throughout that the large mass of the leader relative to the follower results in a negligible acceleration of the leader resulting from repulsion with the follower.

$$\boldsymbol{F}_{\mathrm{C}}(\boldsymbol{X},\boldsymbol{Q}) = \frac{k_{\mathrm{C}} Q_{\mathrm{f}} \boldsymbol{E}_{\mathrm{L}}(\boldsymbol{X},\boldsymbol{Q})}{m_{\mathrm{f}}} \tag{3}$$

The proximity of the follower to the charge structure on the leader means that a mutual capacitance exists between the two objects. This affect is described by the relation between the voltage and the charge on a given object.

$$V_i = k_c \frac{Q_i}{R_i} + k_c \sum_{j=1, j\neq i}^{n} \frac{Q_j}{r_{i,j}} \tag{4}$$

Here, $k_{\mathrm{C}} = 8.99 \times 10^9$ Nm^2/C^2 is Coulomb's constant, R_i is the radius of the i^{th} sphere, and $r_{i,j}$ is the distance between the i^{th} and j^{th} spheres. Throughout this paper, the subscript 1 refers to the follower and subscripts 2 through n refer to the spheres on the charge structure. The relation above can be rewritten into a single matrix equation.

$$\begin{pmatrix} V_1 \\ V_2 \\ \vdots \\ V_n \end{pmatrix} = k_c \begin{bmatrix} 1/R_1 & 1/r_{1,2} & \dots & 1/r_{1,n} \\ 1/r_{2,1} & 1/R_2 & \dots & 2/r_{2,n} \\ \vdots & \vdots & \ddots & \vdots \\ 1/r_{n,1} & 1/r_{n,2} & \dots & 1/R_n \end{bmatrix} \begin{pmatrix} Q_1 \\ Q_2 \\ \vdots \\ Q_n \end{pmatrix} \tag{5}$$

Written in a more compact fashion

$$\boldsymbol{V} = [S]\boldsymbol{Q} \tag{6}$$

where $[S]$ is the elastance matrix.[9] Another expression relating charge to voltage, $\mathbf{Q} = [C]\mathbf{V}$ indicates that the capacitance is the inverse of the elastance matrix.[9]

$$\mathbf{Q} = [S]^{-1}\mathbf{V} \tag{7}$$

The electric field of the leader is the superposition of the individual fields from the charged spheres on the leader craft.

$$\boldsymbol{E}_{\mathrm{L}} = \sum_{i=2}^{n} \frac{Q_i}{r_{1,i}^3} \boldsymbol{r}_{1,i} \tag{8}$$

Here, $\boldsymbol{r}_{1,i}$ is a vector pointing from the i^{th} sphere to the follower craft. The collection of charged spheres on the leader create electrostatic potential well like that shown in Figure 2 according to this equation. Combining with Eq. (3) yields the acceleration of the follower in terms of only the distance between the follower and each sphere and the charges. Henceforth, the follower craft is indicated by the numeral 1 to indicate its position within Eq. (5).

$$\boldsymbol{F}_{\mathrm{C}}(\boldsymbol{X},\boldsymbol{Q}) = \frac{k_{\mathrm{C}} Q_1}{m_{\mathrm{f}}} \sum_{i=2}^{n} \frac{Q_i}{r_{1,i}^3} \boldsymbol{r}_{1,i} \tag{9}$$

This equation can also be interpreted in terms of a superposition of the Coulomb acceleration generated between the follower and each of the charged spheres on the leader.

Incorporating the HCW and drag formulation discussed above, the equations of motion implemented in the controller are

$$\boldsymbol{F}(\boldsymbol{X},\boldsymbol{Q}) = \begin{bmatrix} \boldsymbol{v} \\ \boldsymbol{F}_{\mathrm{C}}(\boldsymbol{X},\boldsymbol{Q}) \end{bmatrix} + [A_{\text{HCW+Drag}}]\boldsymbol{X} \tag{10}$$

CONTROL METHODOLOGY

An optimal control approach is used to control the position of the follower. Previous work used voltage as the control variable for similar scenarios, as this quantity can be sourced directly unlike charge. However, it is clear upon inspection of Eq. (7) that the equations of motion described by Eq. (9) are thoroughly nonlinear in voltage. However, they are linear in the control vector $\boldsymbol{U} = [Q_1Q_2, Q_1Q_3, ..., Q_1Q_n]^T$. A 'charge product' control scheme eliminates the presence of the non-linearities which proved the downfall of the voltage control method. Applying this control vector, Eq. (9) is rewritten.

$$\boldsymbol{F}_{\mathrm{C}}(\boldsymbol{X}, \boldsymbol{U}) = \frac{k_{\mathrm{C}}}{m_{\mathrm{f}}}[r]\boldsymbol{U} \tag{11}$$

The quantity $[r] = [\boldsymbol{r}_{1,2}^T/r_{1,2}^3, \boldsymbol{r}_{1,3}^T/r_{1,3}^3, ..., \boldsymbol{r}_{1,n}^T/r_{1,n}^3]^T$ is defined to remove the summation and simplify later calculations.

The limited size of the plasma wake in which electrostatic actuation is possible motivates the implementation of a tracking formulation. The chosen cost function is that of the classic Linear Quadratic Tracking (LQT) problem.

$$J = \frac{1}{2}\int (\boldsymbol{X} - \boldsymbol{X}_r)^T[Q](\boldsymbol{X} - \boldsymbol{X}_r) + \boldsymbol{U}^T[R]\boldsymbol{U}\mathrm{d}t \tag{12}$$

Here, $\boldsymbol{X}_r$ is the reference trajectory. While an abbreviated, control-only cost function could be simpler to implement, a proscribed trajectory provides a means of better ensuring that the follower does not leave the limits of the plasma wake. The Hamiltonian of the system is

$$\mathscr{H} = \frac{1}{2}\left((\boldsymbol{X} - \boldsymbol{X}_r)^T[Q](\boldsymbol{X} - \boldsymbol{X}_r) + \boldsymbol{U}^T[R]\boldsymbol{U}\right) + \boldsymbol{\lambda}^T\boldsymbol{F}(\boldsymbol{X}, \boldsymbol{U}) \tag{13}$$

Applying the necessary conditions yields

$$\dot{\boldsymbol{X}} = \frac{\partial \mathscr{H}}{\partial \boldsymbol{\lambda}} = \boldsymbol{F}(\boldsymbol{X}, \boldsymbol{U}) \tag{14}$$

$$\boldsymbol{0} = \frac{\partial \mathscr{H}}{\partial \boldsymbol{U}} = [R]\boldsymbol{U} + \left[\frac{\partial \boldsymbol{F}(\boldsymbol{X}, \boldsymbol{U})}{\partial \boldsymbol{U}}\right]\boldsymbol{\lambda} \tag{15}$$

$$\dot{\boldsymbol{\lambda}} = -\frac{\partial \mathscr{H}}{\partial \boldsymbol{X}} = -[Q](\boldsymbol{X} - \boldsymbol{X}_r) - \left[\frac{\partial \boldsymbol{F}(\boldsymbol{X}, \boldsymbol{U})}{\partial \boldsymbol{X}}\right]\boldsymbol{\lambda} \tag{16}$$

The Jacobian of the dynamics with respect to the control is simple given the linear dynamics demonstrated in Eq. (11).

$$\left[\frac{\partial \boldsymbol{F}(\boldsymbol{X}, \boldsymbol{U})}{\partial \boldsymbol{U}}\right] = \frac{k_{\mathrm{C}}}{m_{\mathrm{f}}}\begin{bmatrix}[0]\\ [r]\end{bmatrix} \tag{17}$$

The Jacobian with respect to the states is more complicated. Rather than detail the derivation, the result is provided.

$$\left[\frac{\partial \boldsymbol{F}(\boldsymbol{X}, \boldsymbol{U})}{\partial \boldsymbol{X}}\right] = \begin{bmatrix}[0] & [I]\\ k_{\mathrm{C}}\sum_{i=1}^{n}\frac{U_i}{r_{1,i}^3}([I] - 3\hat{\boldsymbol{r}}_{1,i}\hat{\boldsymbol{r}}_{1,i}^T) & [0]\end{bmatrix} + [A_{\text{HCW+Drag}}] \tag{18}$$

The equations above are combined to yield the well-known optimal control law for the LQT problem. The remaining derivations are passed over, as the relevant, novel pieces have already been explicated through Eqs. (17) and (18).

$$\boldsymbol{U}^* = -[R]^{-1}\left[\frac{\partial \boldsymbol{F}}{\partial \boldsymbol{U}}\right]^T([K]\boldsymbol{X} - \boldsymbol{s}) \tag{19}$$

Here, $[K]$ is a numerically precomputed gain matrix and $\boldsymbol{s}$ is related to the reference trajectory. Note that the system is not considered Linear Time-Invariant (LTI), so the Jacobians listed above are recomputed at each timestep.

RESULTS & DISCUSSION

Two cases are explored through simulation — one for which the reference trajectory is simply the nominal follower position and another which has a full proscribed trajectory from the position of deployment to the nominal. For both cases, the orbit elements of the leader are $[7000\text{km}, 0, 0^\circ, 0^\circ, 20^\circ, 0^\circ]^T$. A nominal separation distance of 1 m in the along-track direction is chosen to fit the requirements of a DPCA mission. Both scenarios provide an initial velocity which simulates some sort of deployment mechanism.

The size and mass of the leader craft were based roughly on the Iridium spacecraft to provide a reasonable baseline for a LEO mission. The follower is assumed to be a spherical craft small enough to fit within the wake of the leader. To simulate the effects of the wake on atmospheric drag, the drag coefficient of the follower is nulled.

Table 1. System Physical Parameters

Parameter	Leader	Follower
Area (m^2)	0.5	0.008
Mass (kg)	1000	1
Coefficient of Reflectivity	1	1
Coefficient of Drag	2.2	0

Solar Radiation Pressure (SRP) is included as an unmodeled perturbation. Both drag and SRP vary as they pass in and out of sunlight. Drag is varied sinusoidally by $\pm 30\%$, while SRP is cut completely in shade. These simplified models are described in greater detail in Table 2. Note that, along with SRP, the variation in atmospheric density is unmodeled.

Table 2. Simplified SRP and Drag Models

SRP	Drag
$C_\text{D} = \begin{cases} C_\text{D} & 0 \leq \nu < \pi \\ 0 & \pi \leq \nu < 2\pi \end{cases}$	$\rho = \rho_0(1 + 0.3\text{sin}(\nu))$

Due to these unmodeled changes in SRP and drag, a neighboring optimal controller is implemented on the system.

Case 1

The first scenario deploys the follower from the leader places the reference trajectory at the point [0 m, -1 m , 0 m, 0 m/s, 0 m/s, 0 m/s]^T. The physical parameters of the electrostatic actuation system are provided in Table 3.

Table 3. Case 1 Design Parameters

Parameter	Value
V_{f_i}	100 V
n	3
r_cs	1 m
r_s	0.25 m

The HCW follower position is provided in Figure 3. Initially, the follower is deployed from the leader with a velocity in only the along-track direction of -0.1 mm/s. This value was tuned to provide a reasonably fast convergence. However, the reference trajectory defined previously is such that the controller battles between correcting its positions and velocities. For this reason, it fluctuates significantly before coming to

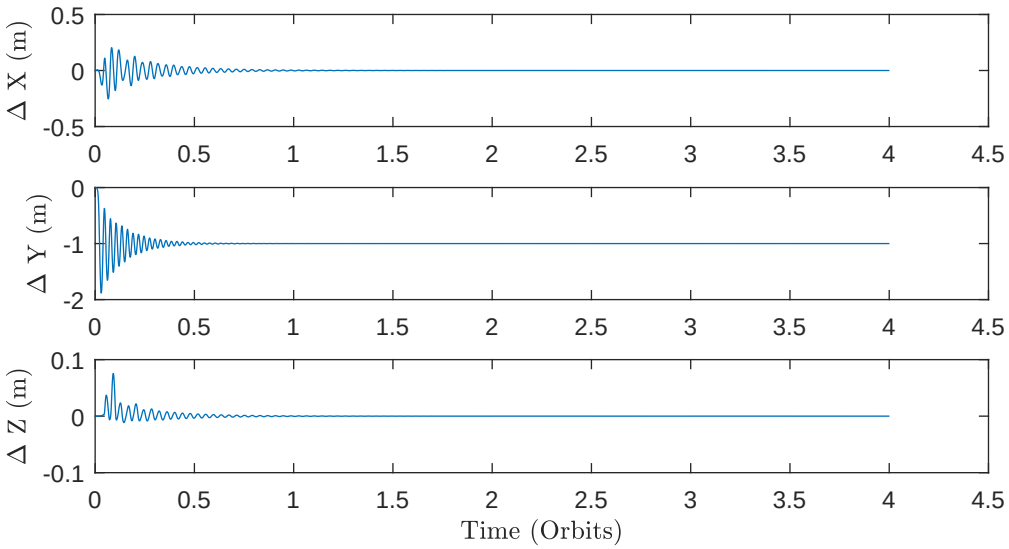

Figure 3. HCW-frame follower position for Case 1

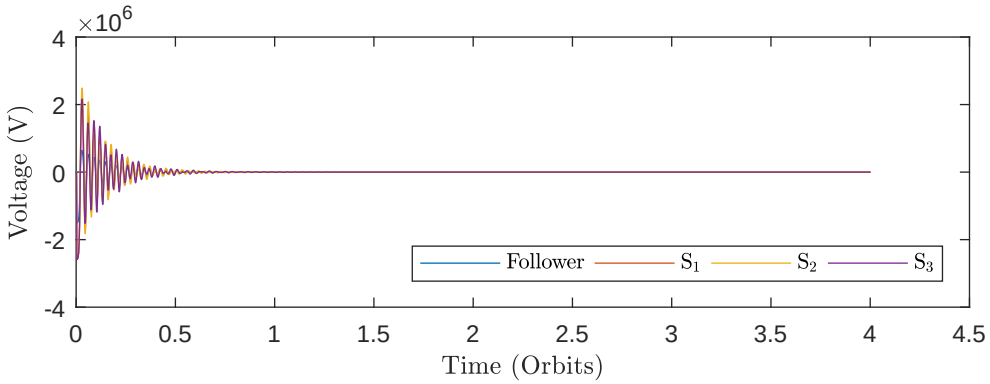

Figure 4. Control voltage for Case 1

the nominal position. The unmodeled perturbations provide the controller with additional difficulty. The HCW-z oscillations result because this direction is coupled to the others through the Coulomb acceleration.

The voltage required by the control for Case 1 is shown in Figure 4. This quantity is calculated from the control vector using Eq. (6). Note that the required voltage is extremely large. For reference, ongoing investigations indicate that electrostatic actuation cannot be performed using even kilovolt levels of charging due to a collapse in the plasma wake. This result motivates the use of an alternate reference trajectory.

A challenge in designing this control system — especially with this first case — is that the control is a function of the separation between the leader and follower crafts. This is unique among modern control methods which typically use independent actuators like thrusters. The challenge is introduced in tuning gains. The control gain matrix $[R]$ must be small such that a great deal of charge can be sourced to prevent the follower craft from drifting away and being lost as the Coulomb acceleration between the craft drops off as the inverse square of the separation distance. However, this makes it difficult to generate any subtle acceleration between the two craft, as the controller is given a great amount of license in sourcing voltage.

This complication is demonstrated by Figure 3. Note that the HCW positions do not visibly change after

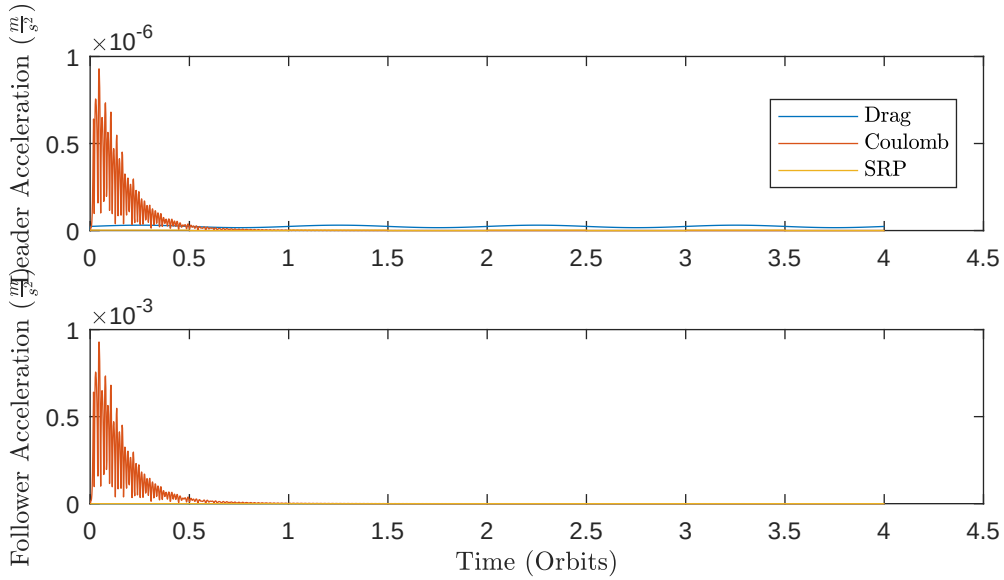

Figure 5. Drag, Coulomb, and SRP acclerations on the leader and follower crafts for Case 1

the system has settled, despite the presence of unmodeled perturbations which change on the timescale of half an orbit. This is because a large amount of voltage is immediately sourced when the follower position deviates from the nominal. These voltages cannot be seen on the scale of Figure 4, but are still larger than the kilovolt limit discussed previously.

Figure 5 shows the magnitudes of the accelerations in the system on both the leader and follower. The controller is designed so that the drag acceleration on the leader is canceled by the Coulomb repulsion on the follower. However, the large initial offset from the reference upon deployment results in the follower's Coulomb acceleration to greatly exceed the leader's drag. Previous work implementing voltage control used much smaller initial offsets and did not result in such large accelerations. However, the necessity for a small [R] matrix results in an extremely over-damped system. This results in large commanded voltages as seen above and clearly compromises the plausibility of the system. This motivates the application of a new reference trajectory.

Case 2

Given the shortcomings of Case 1, the second scenario was designed to gradually push the follower craft from its initial position to the nominal. A trajectory making use of the natural dynamics between the two craft was chosen to reduce the control effort. As discussed previously, it is assumed that some deployment mechanism provides an initial velocity to the follower as it is deployed from the leader. The goal of the general mission described herein is to push the leader back from the follower to some nominal position without deviating significantly. The HCW formulation specifies a condition on a closed relative orbit. Without developing the formulation required to justify, this condition is that the offset in the HCW-x direction must be null. This is equivalent to saying that the follower and leader craft inertial orbits must have identical semimajor axes. This means that an initial HCW-x velocity will generate a drift between the two craft which will naturally push them apart.

The HCW State Transition Matrix (STM) is used to map a given position back to the initial state of the follower. While the STM applies linearized gravity to the nonlinear simulation, the extremely close proximity between the leader and follower craft minimizes the resulting error.

$$\boldsymbol{X}_0 = \begin{pmatrix} \boldsymbol{r}_0 \\ \boldsymbol{v}_0 \end{pmatrix} = [\Phi(t_0,t)]\boldsymbol{X}(t) = \begin{bmatrix} [\Phi_{rr}] & [\Phi_{rv}] \\ [\Phi vr] & [\Phi vv] \end{bmatrix} \begin{pmatrix} \boldsymbol{r}(t) \\ \boldsymbol{v}(t) \end{pmatrix} \tag{20}$$

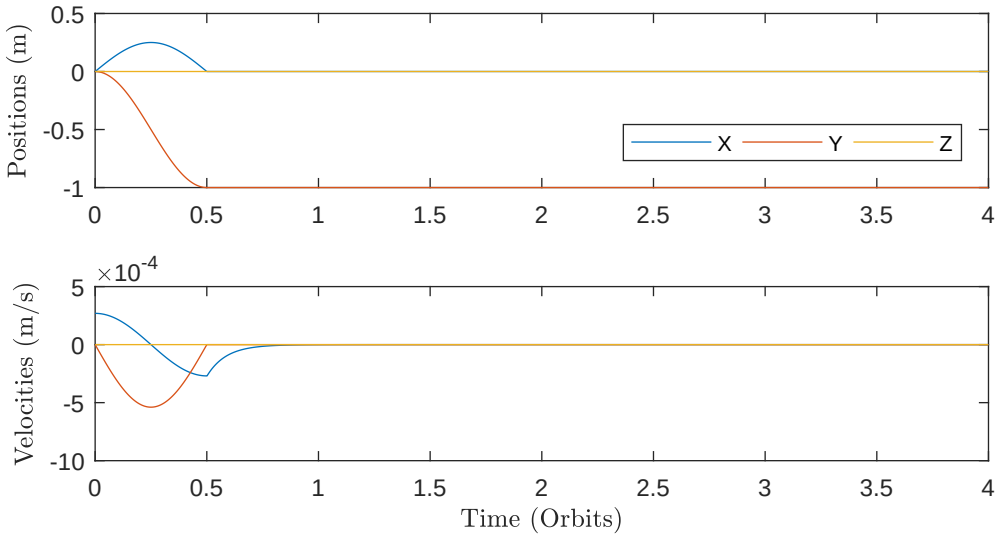

Figure 6. Reference Trajectory for Case 2

Table 4. Case 2 Design Parameters

Parameter	Value
V_{f_i}	500V
n	3
r_{cs}	0.1m
r_s	0.1m

Equation (20) can be rearranged to solve for the initial velocity given an initial and final position. Expanding Eq. 20 yields two equations.

$$\boldsymbol{r}_0 = [\Phi_{rr}]\boldsymbol{r}(t) + [\Phi_{rv}]\boldsymbol{v}(t) \tag{21}$$
$$\boldsymbol{v}_0 = [\Phi_{vr}]\boldsymbol{r}(t) + [\Phi_{vv}]\boldsymbol{v}(t) \tag{22}$$

Solving the first equation for $\boldsymbol{v}(t)$ and rearranging gives an expression to calculation $\boldsymbol{v}_0$ given the initial and final positions. Importantly, the final velocity must remain free, as the other three parameters are fixed.

$$\boldsymbol{v}_0 = [\Phi_{vr}]\boldsymbol{r}(t) + [\Phi_{vv}][\Phi_{rv}]^{-1}(\boldsymbol{r}_0 - [\Phi_{rr}]\boldsymbol{r}(t)) \tag{23}$$

The initial velocity calculated using Eq. (23) and used to generate the reference trajectory shown in Figure 6 is $\boldsymbol{v}_0 = [0.270, 0, 0]^T$ m/s. Note that, unlike the previous trajectory used, the HCW-y velocity is null. The velocity was chosen such that the nominal position is achieved in half an orbit period. As mentioned previously, the final velocity must remain free to solve Eq. (20) for $\boldsymbol{v}_0$, resulting in a non-zero velocity when the follower reaches the nominal position. Rather than immediately demand that the control cease all motion in the HCW-x direction — which would demand a great amount of control — the trajectory is altered to exponentially decrease the HCW-X velocity throughout another 0.25 orbits.

Table 4 provides the parameters used in the electrostatic actuation system for Case 2. Note that only the initial follower voltage is changed for this case. It was increased to decrease the total control needed throughout the simulation.

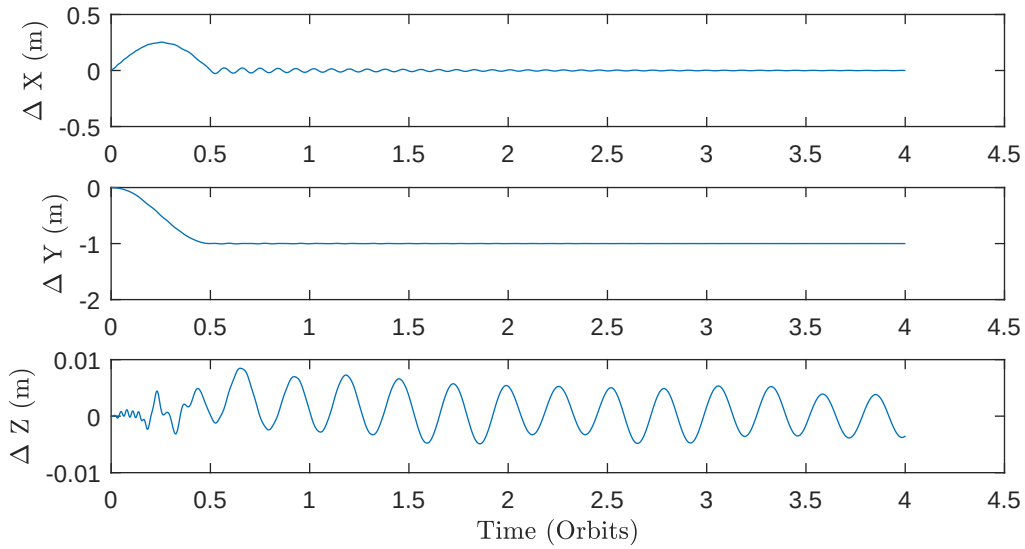

Figure 7. HCW-frame follower position for Case 2

Figure 7 shows the HCW position of the follower throughout the simulation. Note that the initial position oscillations in the HCW-x and -y directions seen in Figure 3 are minimized in this latter case. Note here that the HCW-x and HCW-z fluctuations — which are coupled — persist far longer than those in HCW-y. This is due to the modification in the [Q] matrix, which places a heavier weight on settling in-plane motion than that in HCW-z. Additionally, a much larger [R] matrix in this case limits the amount of voltage sourced by the controller, as seen in Figure 8.

The benefit of designing a reasonable trajectory demonstrated by the HCW positions in Figure 7 is also demonstrated by the control voltage shown in Figure 8. Of note is the much smaller sourced voltage than that in Figure 4. Unfortunately, despite the exponential dropoff discussed above and shown in Figure 6, a great deal of control is required to bring the HCW-x velocity to zero and to minimize the resulting motion due to coupling to other directions.

It is seen in Figures 7 and 8 that the affects of the unmodeled SRP and drag variations are being accounted for. Additionally, Figure 9 shows a much smaller difference between the drag acceleration on the leader craft and the Coulomb acceleration on the follower craft.

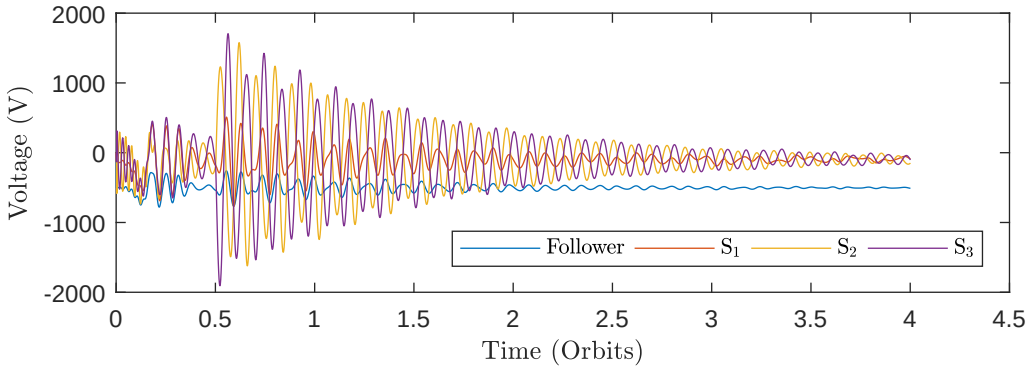

Figure 8. Control voltage for Case 2

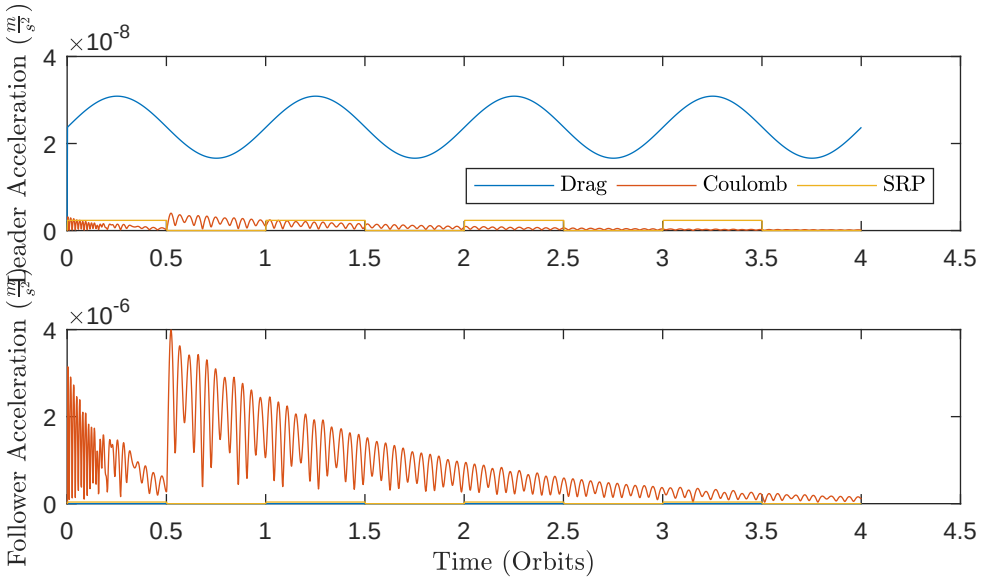

Figure 9. Drag, Coulomb, and SRP acclerations on the leader and follower crafts for Case 2

While this trajectory — chosen to minimize control usage — proved much less expensive than that in Case 1, it still required more voltage than desired for electrostatic actuation in LEO plasma wakes. One possible reason for this is that, though the control effort to remain on the reference trajectory is small, the natural dynamics result in a large relative velocity at the nominal position which must then be negated through the use of control.

CONCLUSION & FUTURE WORK

Coulomb actuation is applied to close-proximity leader-follwer formation with the goal of maintaining relative position with high precision. The DPCA mission concept is used to guide the generation of feasible parameters. A formulation of the Coulomb acceleration is provided using MSM, and is then used within an optimal control framework to generate an optimal control law. Simulations are performed with unmodeled perturbations and various reference trajectories and control effort is assessed resulting in the conclusion that making use of the natural system dynamics is far more fuel-efficient. Future work will investigate the use of alternate trajectories and control strategies to further reduce the maximum control voltage of the system.

REFERENCES

[1] Gordon Roesler. Robotic Servicing of Geosynchronous Satellites (RSGS) Proposers Day Briefing prepared for Robotic Servicing of Geosynchronous Satellites (RSGS) Proposers Day. 2016.
[2] Niels H. Roth, Ben Risi, C. Cordell Grant, and Robert E. Zee. Flight Results from the CanX-4 and CanX-5 Formation Flying Mission. *4S Symposium*, (1):1–15, 2016.
[3] D E Hastings. A review of plasma interactions with spacecraft in low Earth orbit. *Journal of Geophysical Research*, 100(A8):14457–14483, 1995.
[4] S. L. Durden, P. R. Siqueira, and S. Tanelli. On the use of multiantenna radars for spaceborne doppler precipitation measurements. *IEEE Geoscience and Remote Sensing Letters*, 4(1):181–183, 2007.
[5] S. Tanelli, S. L. Durden, and M. P. Johnson. Airborne Demonstration of DPCA for Velocity Measurements of Distributed Targets. *IEEE Geoscience and Remote Sensing Letters*, 13(10):1415–1419, 2016.
[6] Benoit Durand de Gevigney, Thomas Sunn Pedersen, and Allen H Boozer. Debye screening and injection of positrons across the magnetic surfaces of a pure electron plasma in a stellarator. *Physics of Plasmas*, 18(1):013508, 2011.
[7] Elvis D. Silva. A Formulation of the Clohessy-Wiltshire Equations to Include Dynamic Atmospheric Drag. *AIAA/AAS Astrodynamics Specialist Conference*, (August), 2008.
[8] Andrew T. Harris, Christopher Petersen, and Hanspeter Schaub. Linear Coupled Attitude-Orbit Control Through Aerodynamic Forces. *2018 Space Flight Mechanics Meeting*, (January):1–13, 2018.

[9] William R. Smythe. *Static and dynamic electricity*. McGraw–Hill, 1968.